

Chapter 2

Diagnostic of Peak Laser Intensity by Electron and Positron Production from Laser Plasma



A. Andreev, Chen Lan, and Zs. Lecz

Abstract It is known that in the small quantum parameter regime the Breit-Wheeler electron-positron pair creation cross section is extremely sensitive on the photon energy and on the background field. We present the dependence of positron yield on laser intensity in shaped laser under/over dense (gas/foil) plasma interactions with the help of analytical modeling and PIC simulations. This allows for establishing in situ laser intensity diagnostic by measuring the positron yield in experiments where multi PW lasers are used.

2.1 Introduction

Despite of the great success in the development of multi PW laser systems, [1] the development of diagnostics used to determine its ultra-high peak has been left to be explored. A relatively simple method is needed to find the peak intensity of a laser pulse during the experiment at full energy level near the laser focal spot. Usually, the peak intensity in the focal volume is determined from the characteristics such as pulse duration and focal spot size separately measured at significantly lowered pulse energy. Therefore, the estimated peak intensity can be largely different from the correct value. The low accuracy of this method makes it difficult to compare experimental results achieved at different laser facilities [2]. For example, recompression errors, that are specific for the CPA technique can lead to significant errors in determination of the pulse duration in the focal region. Thus, the development of alternative methods for the estimation of focused intensity directly in the experimental chamber is of great importance for investigations in super strong laser field science. A variety of different indirect techniques to diagnose the peak intensity was already proposed in [3–10]. One of the techniques involves laser irradiation of a low-density noble gas

A. Andreev (✉)
SPbSU, Saint Petersburg, Russia

MBI, Berlin, Germany

A. Andreev · C. Lan · Zs. Lecz
ELI-ALPS, Szeged, Hungary

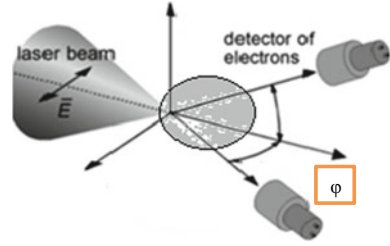
target and the registration of multiple-stage ionization of the gas [3, 4], and another concerns analysis of the accelerated electrons and back Thomson/Compton scattering [5, 6]. Most of these methods work in relatively narrow ranges of laser intensity and require external beams of nearly mono-energetic electrons or ions of prepared in a well-defined ionization state. This, strongly narrows the possibilities of using such diagnostic techniques because of the required specifications of corresponding additional particle source. Therefore, it has been awaited to find other methods of to determine the laser peak intensity in a focal volume. In this paper, we analyze some more simple and inexpensive variants of such diagnostics based on electron and positron production from laser plasma.

2.2 Diagnostics of Peak Laser Intensity Based on the Measurement of Parameters of Electrons Emitted from Laser Focal Region

The method developed in [7–10] is based on the measurement of energy spectrum of electrons, directly accelerated by a laser pulse from rarefied gas or an ultra-thin foil in the beam waist. This allows one to omit impact from additional spurious plasma effects and directly connects laser pulse parameters with electron angular-spectral distributions. Direct electron acceleration by a focused laser pulse was studied theoretically in numerous publications (see for example [11]) and experimentally observed just in a few studies [12, 13]. In the publication [7], we study an approach, proposed recently [9]. This method is based on the measurement of energies of electrons, accelerated in the focal volume that carry residual energy comparable with the oscillation energy in the intense laser field. The electrons are created via the ionization process of a low-density gas target (their concentration is low enough to make the effects stemming from both the Coulomb interactions between the charged particles and the collisions between them negligible, as well as acceleration by plasma wake fields). Dynamics and energy distribution of electrons expelled from the interaction area are determined by the laser pulse parameters. Consequently, measurement of the particle energy distribution can serve as an instrument of diagnosing the laser pulse parameters in the focal spot, in particular the maximum intensity. It was shown that for a certain period of time the electron remains trapped by the laser pulse and moves with it along the pulse propagation axis. This approach (see Fig. 2.1) does not require any additional target or a particle beam and can be used on an everyday basis for a fast control of the laser system.

In the research [7], we realized this method by diagnosing the peak intensity based on the detection of the angular distribution of electrons accelerated in near-vacuum directly by the field of tightly focused relativistic laser pulse. Using the analytical test particle method and 2D PIC simulations, the spatial and energy distributions of scattered electrons from the focal volume have been studied with different sets of laser pulse parameters. The results of numerical calculations and analytical expressions

Fig. 2.1 Simulation and experimental setup [7]



are presented in Fig. 2.2, where we considered propagation of a Gaussian-shaped laser pulse with intensity $I \geq 10^{19}$ W/cm² in the Ar plasma of ion density $n_i = 10^{14}$ cm⁻³ along the Y-axis. The dependence of the average charge of Ar atoms on the laser intensity was taken from the ADK model. The pulse duration (t_L) is $t_L = 40$ fs and the beam diameter (d_L) is $d_L = 10 \mu\text{m}$. The size of the simulation box was $100 \times 100 \mu\text{m}^2$ and the grid size was 40 nm. The time step was 0.1 fs and 20 particles per cell were taken.

The particles were emitted with high residual momentum mostly in a relatively narrow range of the angles from the beam axis. With the growth of the peak intensity, this direction of electron emission moves toward this axis. At the same time in the considered range of peak intensities (below 5×10^{19} Wcm⁻², not shown in Fig. 2.2), the electron spatio-energetic characteristics are found to be weakly dependent on the laser transverse energy distribution. This allows for monitoring the peak intensity of the laser radiation by measuring the angular spectra of high energy electrons. The experimental measurements [7] of the angular distribution of electrons being exposed to the focused high power femtosecond laser radiation with a low density helium gas were found to be in good agreement with the calculation results. We have

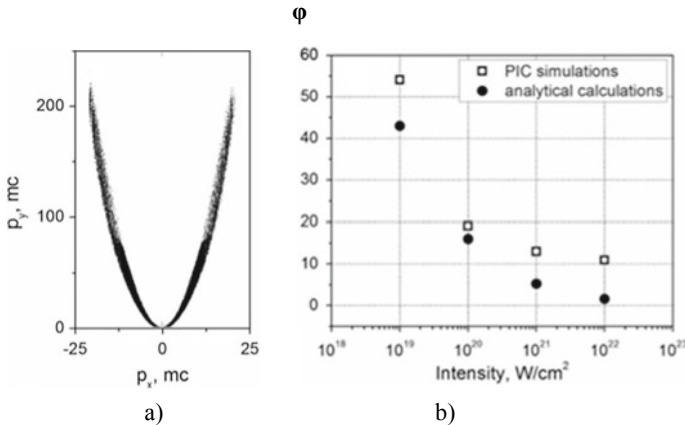


Fig. 2.2 **a** The momenta distribution of electrons propagating out of the focal volume at laser intensity 10^{20} W/cm²; **b** The position of the maximum of angular electron density distribution (open squares—simulation results) and angle ϕ of single electron propagation in a plane wave (closed circles—analytical results) [7]

demonstrated that, with the use of our technique, the peak intensity may be estimated and controlled in each laser shot.

2.3 Diagnostic of Peak Laser Intensity by Pair Production in Low Density Plasma

The method considered above is based on the measurement of energy spectrum of electrons, directly accelerated by a laser pulse from rarefied gas or an ultra-thin foil in the beam waist. This allows one to directly connect laser pulse parameters to electron angular spectral distributions. At ultrahigh intensity ($> 10^{22}$ W/cm²), this technique cannot have a high accuracy mainly because of the radiation reaction, or photon recoil effect. Moreover, secondary electrons are also produced via pair creation, which can change the angular distribution of detected electrons. In this paragraph, we consider another straightforward diagnostic of the laser intensity based on the detection of the number and angular distribution of positrons generated from low density plasma, which is created from residual gas in experimental target chamber. A moderate intensity laser pre-pulse can produce such plasma. In such medium, the electrons (shown by red) are directly accelerated in a laser caustic by the field of a focused ultra-intense laser pulse, which is reflected at some point of a focusing parabolic mirror M.

The dominant process responsible for pair creation in our conditions is the multi-photon Breit-Wheeler process, which has a very sharp intensity threshold slightly above $I = 10^{22}$ W/cm². Below this threshold no pairs are created, but, above the threshold, the number of pairs increases extremely fast with laser intensity. The highly sensitive dependence of the positron detection efficiency on the laser intensity makes the precise diagnostic possible. In [14], we proposed a process to diagnose the laser intensity by measuring the positron yield. The process consists of two steps. First, the electrons (red dot in Fig. 2.3) with relatively low energy are accelerated by the axial electric field generated from the reflected part (violet lines) of the incident shaped laser pulse (blue lines) by dented mirror M, which is approximated by two crossing pulses [8] with a small angle of propagation (see Fig. 2.3). In the second step, the accelerated electrons then collide with the rest of the laser pulse in order

Fig. 2.3 Schematic diagram of setup

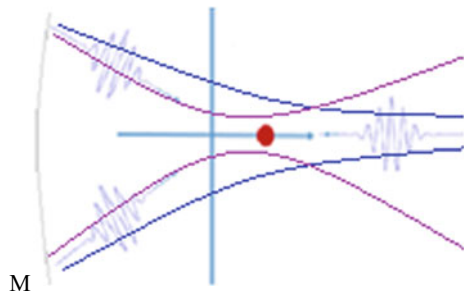
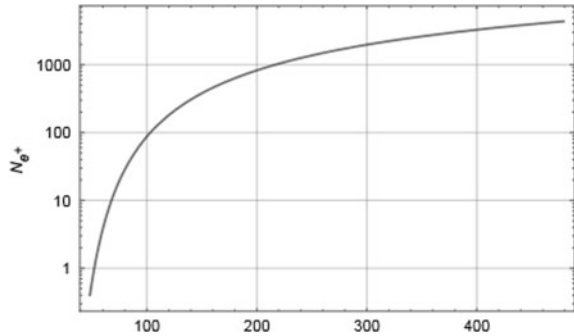


Fig. 2.4 The dependence of positron-number with $a \in [48, 480]$ in the LCFA, where laser pulse duration is 10 fs, $\Delta\phi = 23.56$ and $N_{e^-} = 100$



to produce electron-positron pairs. The laser intensities at each step satisfy a certain relation, which is appropriate and can be prepared by shaping a laser with optical apparatus. The electrons are supposed to be located on the horizontal axis with small initial energy. Thus, the acceleration can be realized by a tightly focused laser beam.

To demonstrate this process, it is enough to consider only sinusoidal fields [15]. The electron energy can be written as: $\varepsilon_{\max} = mc^2(1 + 8a^2)$, where a is the dimensionless magnitude of the vector potential. In our case, $a = eE/m\omega c \gg 1$, which is also known as local constant field approximation (LCFA), see e.g. [16]. Here E and ω are strength and frequency of laser field, $a = 6\sqrt{I_0}[10^{20} \text{ W/cm}^2]\lambda_0[\mu\text{m}]$. In LCFA all fields can be regarded as a constant crossed field, thus if all parameters are the same, the shapes of the field would not affect the differential rate too much. The corresponding probability P_2 for constant crossed field can be represented via the approximate formula of the differential rate $J_{\nu e}$ (see for example [16, 17]): $P_2 \approx 0.5 \times (a\Delta\phi)^2 \times (3\alpha^2/16\chi_e) \times \ln(1 + \chi_e/12) \times \exp(-16/3\chi_e) \times (1 + 0.56\chi_e + 0.13\chi_e^2)^{1/6}$, where fine-structure constant in the used units $\alpha = e^2$, $\chi_e = a \times 10^{-4} \times [-6.1 + 2.45a + 6.17\sqrt{(1 + 0.16a^2 - 0.79a)}]$ and $\Delta\phi$ are the formation phase length, see [17]. The differential rate $J_{\nu e}$ is valid in the range $\chi_e \in (1, \infty)$. Thus, the positron numbers in one pulse can be estimated by $N_{e^+} = P_2 N_{e^-}$, where N_{e^-} is the initial number of electrons, see Fig. 2.4.

Here the probability of pair production is carried out in LCFA, i.e. the background field is regarded as constant crossed field. However, as several authors reported, see e.g. [18–20], the production rate may be enhanced due to the finite extent of a laser field. Therefore, the finite size effect of the diagnostics of intensity should be taken into account in order to increase the accuracy of this method. These represent the program for future research.

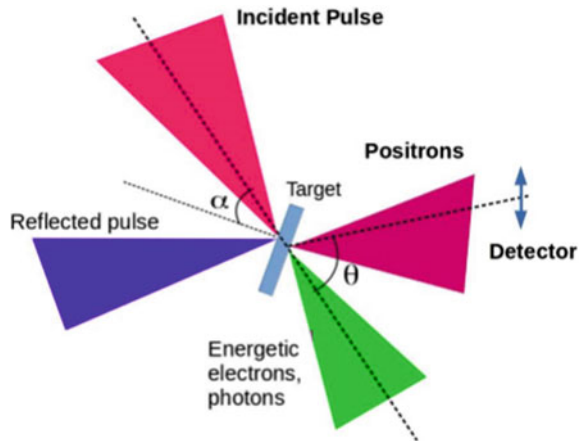
2.4 Diagnostic of Peak Laser Intensity by Pair Production from Thin Foil Target

In the paper [21], we propose another simpler diagnostic of the laser intensity based on the detection of the number and angular distribution of positrons generated from

thin foil, which is a usual target in recent experiments. A moderate intensity laser pulse, or a prepulse, can produce the desired density distribution at the surface of a flat foil target. In such medium, the electrons are directly accelerated by the field of focused ultra-intense laser pulse, which at some point is reflected in the overdense region of the expanded plasma. In contrast with the previous schemes, in our method a single laser pulse is sufficient to generate pairs instead of two counter propagating pulses.

Figure 2.5 shows that in our numerical experiment, the high power laser pulse (shown by red) is focused on the surface of a thin foil target. The generated positrons are well separated from all other secondary radiations and are detectable at angle θ with respect to the laser axis. The dominant process responsible for the pair creation in our conditions is also the Breit-Wheeler process, which has a sharp intensity threshold. Below this threshold no pairs are created but, above the threshold, the number of pairs increases extremely fast with laser intensity. We used the 2D EPOCH simulation code to demonstrate the dependence of positron number on the laser intensity [22]. The P-polarized laser pulse has Gaussian temporal (longitudinal) and transversal profiles with 30 fs (FWHM) duration and $3 \mu\text{m}$ focal spot diameter. The incident angle was 30° and $n_0 = 350n_{cr}$ is used for the maximum plasma density. The preplasma has an exponential density profile with a scale length of $L_n = 0.5 \mu\text{m}$ and the total preplasma length of $L_p = 2 \mu\text{m}$. The thickness of the uniform plasma (unperturbed target) was $1 \mu\text{m}$. The simulation box was $16 \mu\text{m}$ long and $16 \mu\text{m}$ wide which is resolved by 4000×4000 grid cells. In each cell, 20 macro-particles of electrons and ions were initially loaded. The target material was gold and 30^+ charge state is used. The length of the preplasma is important not only for seeding the pair creation but also for determining the acceleration path of electrons. In this particular case, the electrons are accelerated via the direct laser acceleration mechanism [20], which provides electron energies high enough to emit gamma photons with several hundred MeV energy. The propagation of low energy ($< 75 \text{ meV}$) photons are not included in the simulation, because they do not contribute to the pair creation, but their

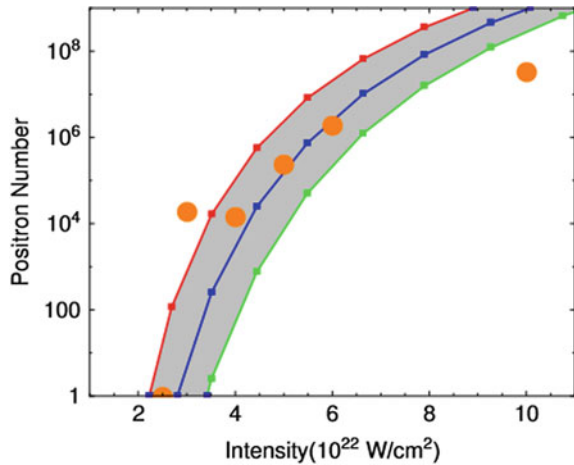
Fig. 2.5 Basic setup of our simulations and of possible experiments [21]



recoil on the emitting electrons is always calculated in the code for consistency. The photons are generated inside the preplasma when the fast electrons collide with the reflected pulse. During the pulse reflection, the positive amplitude of the laser field is responsible for the pair creation. The electron-positron pairs are generated during less than a quarter laser period, and the pairs will be separated by the positive electric field. The positrons acquire a significant transversal momentum and are deflected with a wide angular spread in a direction almost perpendicular to the original direction of the incident pulse. The large angular spread can be attributed to the large energy spread of photons which are emitted according to the quantum synchrotron function. The laser electric field deflects lower energy positrons because they are less relativistic and their initial momentum is smaller. After the pulse is fully reflected, we count the number of positrons in the simulation domain. The results are presented in Fig. 2.6, where for analytical calculations, different electron cut-off energies (γ_{\max}) are considered.

In Fig. 2.6, the number of positrons calculated from our analytical model (see [21]) are shown by blue squares (joined by straight lines) integrated for all γ up to $\gamma_{\max} = 5a$, by green up to $\gamma_{\max} = 4a$ and by red up to $\gamma_{\max} = 6a$. The large round marks show the simulation results. The positron number can be determined with high accuracy by a standard experimental technique. Because of this sensitive dependence of the positron detection efficiency, the very precise diagnostic becomes possible. At lower intensities, pairs can be generated via the Bethe-Heitler process, which involves the collision of bremsstrahlung photons with highly charged high-Z ions using much thicker targets ($\sim 100 \mu\text{m}$ or more) [23]. In this case, the positron number increases very slowly with laser intensity, therefore the precision cannot be high enough for diagnostics.

Fig. 2.6 The dependence of total number of positrons on laser intensity [21]



2.5 Conclusion

In this paper, we present some possible methods to determine laser peak intensity in the focal volume, based on electron acceleration or positron production from laser plasma interactions. In the case of high power lasers well below the PW level, the measurement of electron energy spectra is relevant, while near or above this level the positron count can be used to estimate the peak intensity. It was shown that, by using the production of positrons from different targets irradiated by high intensity laser pulses, one can determine the laser intensity in the range above 10^{22} W/cm² till 10^{25} W/cm², and the peak intensity can be determined with the accuracy up to $\sim 1\%$.

References

1. G.A. Mourou, T. Tajima, *Science* **331**, 41 (2011)
2. G.A. Mourou, N.J. Fisch, V.M. Malkin, Z. Toroker, E.A. Khazanov, A.M. Sergeev, T. Tajima, B. Le Garrec, *Opt. Commun.* **285**, 720 (2012)
3. A. Link et al., *Rev. Sci. Instrum.* **77**, 10E723 (2006); M.F. Ciappina, S.V. Popruzhenko, S.V. Bulanov, T. Ditmire, G. Korn, S. Weber, *Phys. Rev. A* **99**, 043405 (2019)
4. C. Smeenk, J. Salvaill, L. Arissian L.P. Corkum et al., *Opt. Express* **19**, 9336 (2011); M.F. Ciappina, S.V. Popruzhenko, *Laser Phys. Lett.* **17**, 025301 (2020)
5. J. Gao, *J Appl. Phys. Lett.* **88**, 091105 (2006); O. Har-Shemesh, A. Di Piazza, *Opt. Lett.* **37**, 1352 (2012)
6. W. Yan et al., *Nat. Photon.* **11**, 514 (2017)
7. M. Kalshnikov, A. Andreev, K. Ivanov et al., *Laser Part. Beams* **33**, 361 (2015)
8. O. Vais, S. Bochkarev, S. Ter-Avetisyan, V. Bychenkov, *Quantum Electron.* **47**, 38 (2017); K.I. Popov et al., *Phys. Plasmas* **16**, 053106 (2009)
9. A. Galkin, M. Kalashnikov, V. Korobkin et al., *Phys. Plasmas* **17**, 053105 (2010)
10. K.A. Ivanov, I.N. Tsymbalov, O.E. Vais, S.G. Bochkarev, R.V. Volkov, V.Y. Bychenkov, A.B. Savel'ev, *Plasma Phys. Controlled Fusion* **60**, 105011 (2018)
11. Y. Li, Y. Gu, Z. Zhu et al., *Phys. Plasmas* **18**, 53104 (2011)
12. C. Varin et al., *Appl. Sci.* **3**, 70 (2013)
13. M. Thévenet, K. Leblanc, S. Kahaly et al., *Nat. Phys.* **12**, 355 (2016)
14. A. Andreev et al., *International Conference on Ultrafast Optical Science*, LPI RAS, Moscow, Sept 2019; C. Lan et al., *ELI ALPS SciDay Meeting Szeged*, 12 Oct 2018
15. Y.I. Salamin, C.H. Keitel, *Phys. Rev. Lett.* **88**, 095005 (2002)
16. V.N. Baier, V.M. Katkov, V.M. Strakhovenko, Higher-order effects in external field: pair production by a particle. Technical Report (Novosibirsk State University, USSR 1971); A.I. Nikishov, V.I. Ritus, Quantum processes in the field of a plane electromagnetic wave and in a constant field. I. *Sov. Phys. JETP* **19**, 529–541 (1964)
17. B. King, H. Ruhl, *Phys. Rev. D* **88**, 013005 (2013)
18. T. Heinzl, A. Ilderton, M. Marklund, *Phys. Lett. B* **692**, 250–256 (2010)
19. A. Titov, H. Takabe, B. Kämpfer, A. Hosaka, *Phys. Rev. Lett.* **108**, 240406 (2012)
20. C. Lan, Y. Wang, H. Geng, A. Andreev, *Eur. Phys. J. C* **79**, 917 (2019)
21. Zs. Lecz, A. Andreev, *Laser Phys. Lett.* **17**, 056101 (2020)
22. Z. Lecz, A. Andreev, *PP&CF* **61**, 045005 (2019)
23. H. Chen, S.C. Wilks, J.D. Bonlie, E.P. Liang, J. Myatt, D.F. Price, D.D. Meyerhofer, P. Beiersdorfer, *Phys. Rev. Lett.* **102**, 105001 (2009)